Journal of
Water & Climate Change

Journal of Water and Climate Change Vol 15 No 2, 814 doi: 10.2166/wcc.2024.593

Analysis of the temporal variations in glaciers' surface area in Alaknanda River Basin, Uttarakhand

V. Nunchhani, Sujit Hazarika, Rimum Murtem, Arnab Bandyopadhyay* and Aditi Bhadra

Department of Agricultural Engineering, North Eastern Regional Institute of Science and Technology, Nirjuli (Itanagar), Arunachal Pradesh 791109, India
*Corresponding author. E-mail: arnabbandyo@yahoo.co.in

AB, 0000-0001-6653-250X; AB, 0000-0001-8403-0976

ABSTRACT

This study presented detailed analysis of glacier surface extent in the Alaknanda river basin, Western Himalaya, using Landsat series data, land surface temperature and digital elevation model (DEM). The clean glaciers were delineated using automatic glacier extraction index (AGEI) and the debris-covered glaciers were extracted by utilizing slope and land surface temperature. The generated glaciers map was compared and cross-checked with Randolph Glacier Inventory (RGI v5.0) and sharp google earth image. The reduction in glacier surface area was observed by 367.364 sq. km from 1994 (1150.471 sq. km) to 2015 (783.107 sq. km) at the shrinkage rate of 1.45% per annum. The shrinkage rate was higher from 2006 to 2015 (2.43% per annum) than from 1994 to 2006 (0.78% per annum). The glacier count expanded from 314 (1994) to 360 (2015) due to the fragmentation of individual glaciers. The elevation range of 5000–5500 m above m.s.l. hosted maximum number of glaciers and glacial coverage. The debris-covered glaciers showed deglaciation at the rate of 0.59% per annum from 1994 to 2015. The total area occupied by glacier extent was about 25% of the total basin in the year 1994, 23% in the year 2006 and 17% in the year 2015.

Key words: climate change, debris-covered glaciers, glacier inventory, glacier shrinkage, Himalaya

HIGHLIGHTS

- Mapped clean glaciers using automatic glacier extraction index.
- Mapped debris-covered glaciers by intersecting slope and LST layers.
- Detected shrinkage in glacier surface area during the analysis period.
- Found higher shrinkage rate in the recent period than the older period.
- Observed increase in count of glaciers due to fragmentation.

GRAPHICAL ABSTRACT

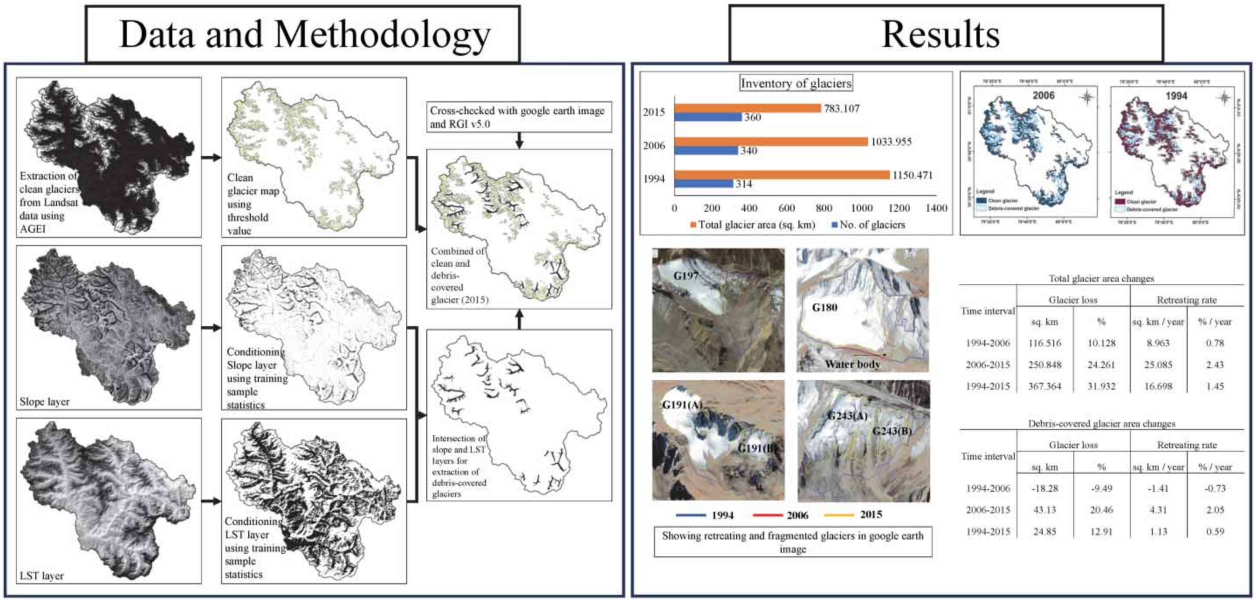

1. INTRODUCTION

The Himalayan glaciers and snow form a huge reservoir of freshwater and are usually called water towers of Asia. They are the source of several major rivers such as the Ganges, Indus, and Brahmaputra. About 30–50% of the annual flow of these river systems is from snow and glacier melt (Aggarwal *et al.* 1983; SAC 2011) and provides water for millions of people, supporting agriculture, hydropower generation, and domestic water supply. However, the Himalayan Mountain glaciers have undergone substantial deglaciation in the recent decades due to an upsurge in the degree of climate change and human interference (Chand & Sharma 2015; Zemp *et al.* 2015). The decrease in glacier surface area and glacier lake outburst are common phenomena that can be observed in the Indian Himalayas (Bajracharya *et al.* 2008; Padma 2020; Dimri *et al.* 2021). Several studies indicate that glaciers in the Himalayas are undergoing rapid retreat (Kulkarni *et al.* 2007; Mir *et al.* 2017; Alam & Bhardwaj 2020), and this will result in adverse effects on the water flow within the major river systems (Bolch *et al.* 2017; Immerzeel *et al.* 2020; Azam *et al.* 2021). Therefore, mapping and monitoring of changes in glacier surface area in a glaciated basin is essential to offer a comprehensive understanding of freshwater availability on both regional and global scale (Kaushik *et al.* 2022).

Accurate glacier outlines are obligatory for analysing changes in glacier surface extent and serve as the main input for most of the glacio-hydrological research and modelling endeavours (Shukla *et al.* 2009). The changes in glaciers are inherently linked to the glacier's mass balance as the positive annual mass balance may increase the glacier extent, whereas the negative mass balance may reduce the glacier size (Keeler *et al.* 2021). Mapping of glaciers also holds immense significance in understanding and the illustration of global climate change (Oerlemans 2005). Observing and monitoring the glacier area changes through field measurement is very difficult in the Himalayan region due to rugged topography and harsh climatic conditions (Mir *et al.* 2017), thus creating a problem in consistent monitoring and collection of data through field techniques. However, applications of remote sensing and Geographic Information Systems (GIS) enable us to collect, process, analyse, and monitor the state of glaciers in inaccessible high mountainous areas, thus benefitting the glaciological community to perform spatial and temporal analyses at different scales, which is valuable for basin-scale glaciological and hydrological modelling (Suresh *et al.* 2023). The temporal and multispectral satellite data offer an alternative approach with considerable potential to map and monitor glaciers over extensive spatial coverage at consistent time intervals (Mir *et al.* 2014). However, the efficacy of automated glacier mapping from satellite multispectral image data is hindered by the presence of debris over the glacier surfaces (Paul *et al.* 2004). The debris complicates the mapping through satellite images due to its spectral resemblance to the lateral and terminal moraines (accumulation of glacial debris such as rocks, soils, and other materials), fluvioglacial deposits (deposits result from glacial meltwater), and the surrounding rocks, and cannot be detected through multispectral classification alone (Paul *et al.* 2004; Bolch *et al.* 2007). Most of the major glaciers in the Western and Central Himalayas are covered with debris in their frontal area, thus restricting the use of automatic band ratio technique for delineation of glacier extent. The supraglacial debris (debris over the glacier surface) can be distinguished from the surrounding by checking the surface temperature as supraglacial debris is often cooler due to underlying ice and by using geomorphometric parameters such as slope and curvature (Bolch & Kamp 2006). Several studies showed promising results for the delineation of supraglacial debris using a combination of automated multispectral classification, surface temperature, and geomorphometric parameters (Paul *et al.* 2004; Bolch *et al.* 2007; Shukla *et al.* 2009; Alifu *et al.* 2016). The analysis also showed that glacier retreats increase supraglacial debris cover (Benn *et al.* 2012; Bolch *et al.* 2012).

High mountain glaciers can be covered with different degrees of debris (Kaushik *et al.* 2022), and the accuracy of delineation of supraglacial debris-covered glaciers depends on the type of debris covered, the threshold value applied in surface temperature, and geomorphometric parameters which vary from basin to basin (Bolch et at. 2007). Therefore, it is necessary to develop a comprehensive basin-scale glacier assessment for each Himalayan basin (Shukla *et al.* 2020). On the basis of the basin scale and the individual glacier level, many researchers have analysed the temporal change in glacier coverage and mass loss in Western and Central Himalaya (Kulkarni *et al.* 2004, 2005, 2007, 2011; Mehta *et al.* 2011; Nainwal *et al.* 2016; Garg *et al.* 2017; Mir *et al.* 2017; Rai *et al.* 2017). Bhambri *et al.* (2011) conducted glacier studies in Saraswati/Alaknanda basin, Garhwal Himalaya, and identified 83 glaciers with an area coverage of $311.4 \pm 9.8\ km^2$ in the year 2006. Among 83 glaciers, 51 glaciers were covered with debris at their frontal areas that accounted approximately 24.6% of the overall glacierized area. In the Upper Alaknanda basin, Central Himalaya, Mishra *et al.* (2023) conducted a glacier inventory and analysed glacier changes spanning from 1994 to 2020 and identified 198 glaciers, covering an area of $354.6 \pm 8.5\ km^2$.

The study of glacier changes in the whole Alaknanda basin, by taking Joshimath as an outlet where Central Water Commission (CWC) measures daily discharge, has not been reported so far. To fill this research gap, the present study was conducted to prepare a glacier map and analyse the temporal variation in glaciers' surface area using remote sensing and GIS techniques in the whole Alaknanda basin by taking Joshimath as an outlet. The information on the variation of glacier changes will help in making informed decisions on water availability in downstream areas, enabling water management, reducing disaster risks such as glacial lake outburst floods, climate change adaptation strategies, and promoting sustainability in the region as these challenges are predominantly linked to the retreat of glaciers. These generated glacier maps will be useful in quantifying the glaciers' melt contribution to the total stream flow of the Alaknanda River at Joshimath as well, as it is the main input for such analysis in any hydrological modelling of glacier module and will be helpful in better understanding the hydrological regime in the region.

2. STUDY AREA

The study area is situated in the Chamoli district of Uttarakhand state in India. It lies between longitudes of 79°10′ E to 79°45′ E and latitudes of 30°30′ N to 31°10′ N encompassing a total land area of about $4,500\ km^2$, and it represents the Eastern part of Garhwal Himalaya (Figure 1). The discharge measuring site of the CWC at Joshimath located at 79°32′50″ E and 30°33′57″ N was taken as the outlet point. The landscape of the basin is marked by undulating topography, profound gorges, and meandering river valleys with elevation ranges from 1,359 to 7,801 m above m.s.l. The basin experiences an average annual rainfall of 1,257 mm with the monsoon typically commencing in June and tapering off by September and heavy snowfall during winter months. Alaknanda River originates at the snout of Satopanth glacier and Bhagirath Kharak glacier and is one of the two headstreams of India's longest river, Ganges. It is important to map and monitor glacier surface changes in the basin for making informed decisions regarding water availability in downstream regions, water resource management, disaster risk reduction such as glacial lake outburst floods, and climate change adaptation strategies.

3. DATA AND METHODOLOGY

3.1. Data

The glacier surface extent was mapped using Landsat series data, land surface temperature, and digital elevation model. The Landsat data of less seasonal and cloud coverage which were usually available in the ablation months (September and October) were obtained from the United States Geological Survey (USGS) website (https://glovis.usgs.gov/). The land surface temperature of the same acquisition date of Landsat series data were downloaded from the EEFLux (Earth Engine

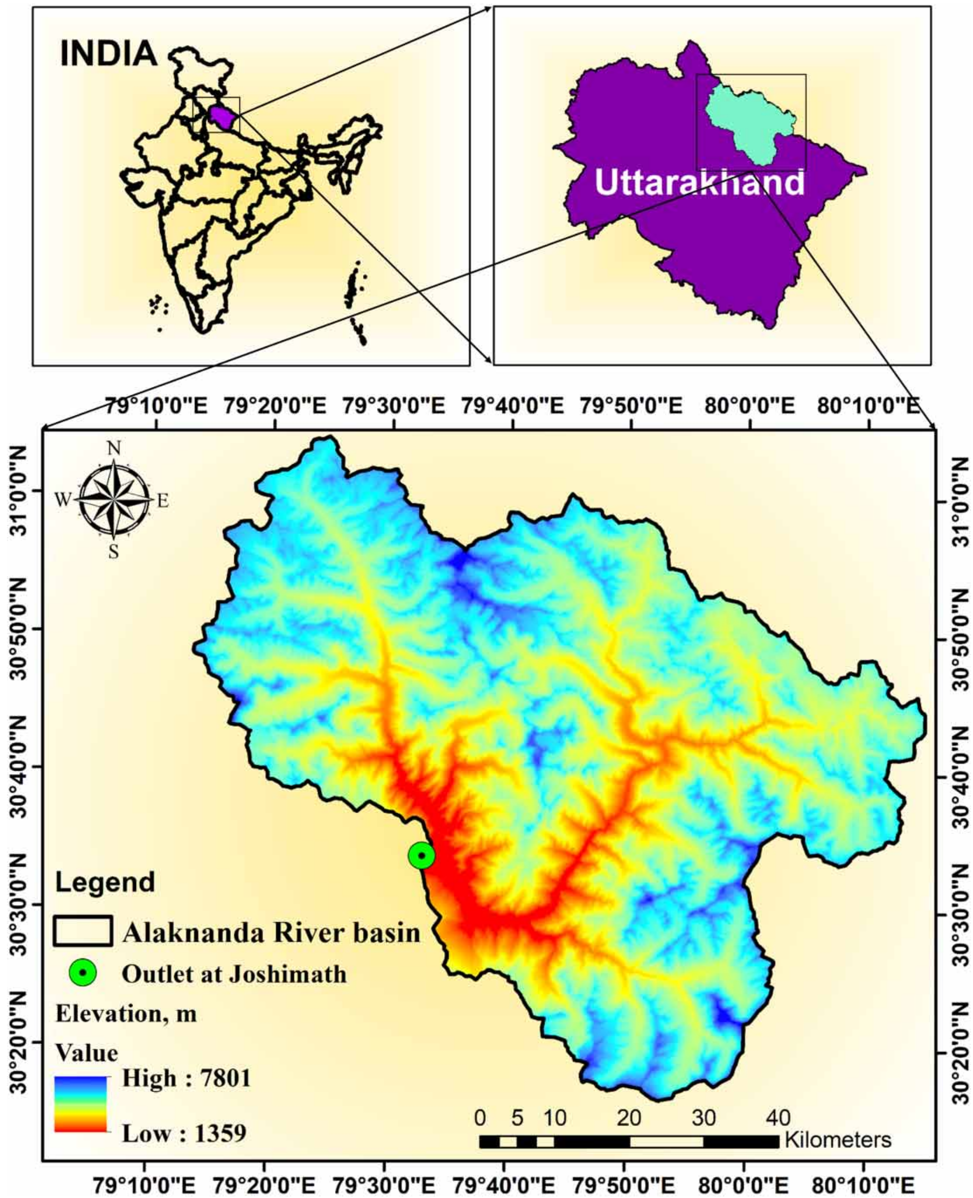

Figure 1 | Location of study area (Alaknanda river basin).

Evapotranspiration Flux) website (https://eeflux-level1.appspot.com/). The SRTM (Shuttle Radar Topography Mission) digital elevation model of 30 m resolution was downloaded (https://dwtkns.com/srtm30m/). For comparison and validation of the generated glacier map, Randolph Glacier Inventory (RGI) version 5.0 of South East Asia was also acquired (https://www.glims.org/RGI/rgi50 dl.html). Besides this, sharp Google Earth images were also incorporated for finalizing the generated glacier map. Table 1 presents information of the acquired Landsat series data.

3.2. Methodology

Glaciers in the Alaknanda River basin are either clean glaciers or a combination of clean and debris-covered glaciers. The automated multispectral glacier mapping methods were not sufficient to delineate the debris-covered glacier surface extent in the basin, and separate remote sensing and GIS techniques were needed for the extraction of debris-covered glaciers. A simplified flowchart for the extraction of glaciers is shown in Figure 2.

Table 1 | Details of Landsat series data acquired

Data	Date of acquisition	WRS path/row	Resolution
Landsat 8 OLI	3 October 2015	145/39	30 m
Landsat 7 ETM	2 October 2006	145/39	30 m
Landsat 5 TM	25 October 1994	145/39	30 m

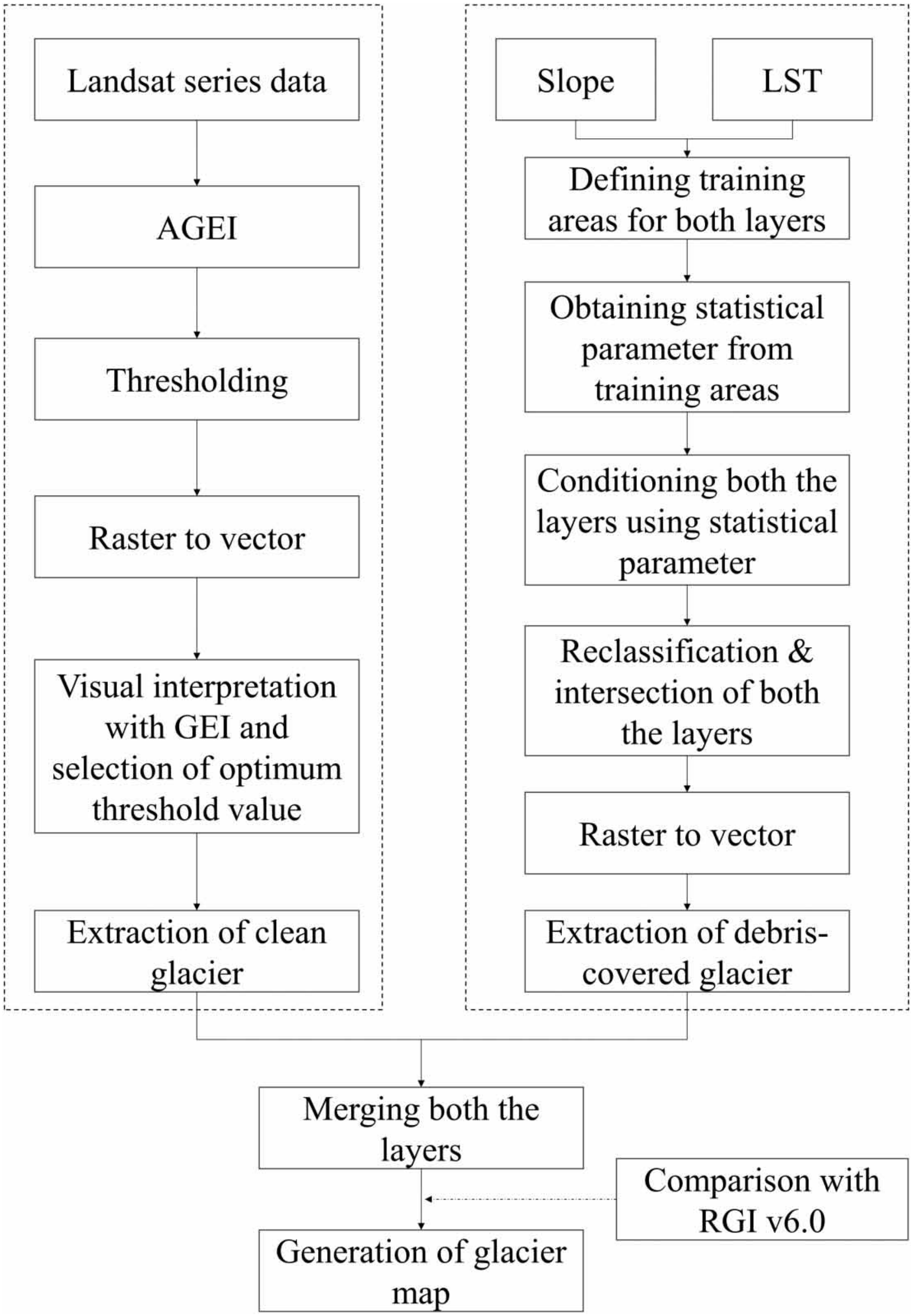

Figure 2 | Processing flowchart for extraction of glacier surface area.

3.2.1. Mapping of clean glaciers

For the extraction of clean glaciers, the automatic glacier extraction index (AGEI) was used. The AGEI was developed to minimize water and shadow classification errors and to enhance the precision of mapping clean glaciers by utilizing Landsat imagery as the commonly used remote sensing methods such as normalized difference snow index (NDSI) and single band ratios of NIR/SWIR and Red/SWIR tend to misclassify the glacier surface area by including water features and bare rock as a glacier, and excluding shadowed glaciers from glacier extent (Zhang *et al.* 2019). The most common problems encountered in mapping glaciers in high mountains are shadows, rocky features, and water features as they show similar spectral reflectance as glaciers, which reduces the accuracy of the glacier surface extent. Therefore, in the present study, the AGEI method is adopted to enhance the precision mapping of the glacier surface extent.

The AGEI is calculated using Equation (1) through ArcMap 10.2 (ArcToolbox → Spatial Analyst Tools → Map Algebra → Raster calculator):

$$\mathrm{AGEI} = \frac{\alpha \mathrm{DN_{Red}} + (1-\alpha)\mathrm{DN_{NIR}}}{\mathrm{DN_{SWIR}}} \tag{1}$$

where $\alpha \in [0,1]$ is a weighted coefficient; DN stands for the raw digital number values; Red, NIR, and SWIR correspond to the red band, near-infrared band, and shortwave infrared band, respectively. The threshold value ranges from 1.5 to 2.5.

A weighted coefficient value (within the range) was applied in the aforementioned equation, and then a single raster image was generated. On the generated single raster image, a threshold value (within the range) was applied, and then a binary raster image was formed. In the binary raster image, the raster value greater than or equal to the threshold value represents the glacier surface, while the raster value lesser than the threshold value represents the non-glacier surface. The binary raster image was converted into vector format using ArcMap 10.2, which was then imported into Google Earth Pro for visual comparison with the high-resolution Google Earth image. The Google Earth image was set as near as possible to the Landsat image acquisition date for better comparison. The most suitable weighted coefficient and threshold value for the study area were then obtained from the visual comparison. In this visual comparison, the coverage of glacial extent was carefully checked, and the inclusion or exclusion of shadowed glaciers, water features, and bare rocks was also cautiously checked.

3.2.2. Mapping of debris-covered glaciers

For the extraction of debris-covered glaciers, two main criteria, namely, the slope of the topography and land surface temperature, were adopted. Typically, the supraglacial debris comes from the adjacent rock walls that lack ice cover which experienced significant weathering (Maisch *et al.* 1999). The debris is carried downhill by the overall glacier flow towards its endpoint, continuing to slide until it encounters a gentler slope where it can accumulate (Paul *et al.* 2004). The debris is usually settled at the glacier frontal area or tongue due to its gentler slope. The land surface temperature enabled to differentiate between the surrounding rocks and supraglacial debris since the temperature of debris over the glaciers was lower than the surroundings due to underlying ice (Bolch *et al.* 2007).

The slope of the basin was generated from the DEM using ArcMap. Firstly, a number of training areas were deliberately selected across several glaciers on both land surface temperature and slope layers. These selected training areas represented the common or typical surface characteristics of debris-covered glaciers. Using the training samples, the statistical parameters of maximum and minimum were derived from both layers. The obtained maximum and minimum values were used to give a condition in the layers by assigning either 0 or 1. The value 1 signified the pixel value which was within the minimum and maximum value range in the layer and 0 signified the pixel value which was out of the range. After assigning 0 and 1, both the layers were intersected and then converted into polygons. The intersected polygon was dissolved and then imported into Google Earth Pro for visual validation. The exposed streams were also utilized to obtain the termini of the glaciers. Some of the misclassified debris covered were also manually eliminated.

3.2.3. Generation of glacier map

After the extraction of the clean ice and debris-covered glaciers, both the layers were merged together and formed a single layer. The merged glacier layer of the year 2015 was compared with RGI v5.0 for validation of the glacier layer extraction methods. The validation was carried out by checking the spatial distribution and the extent of each glacier.

3.2.4. Temporal variation in glacier surface area

The temporal variation in glacial coverage was analysed by dividing the study period into three time slices such as 1994–2006, 2006–2015, and 1994–2015. These time slices were prepared to check any changes in the glacier shrinkage rate/loss in the recent years and in the old years. The glacier areas were further classified based on their size for analysing the relationship between glacier size and glacier shrinkage. The glacier shrinkage area and shrinkage rate were calculated as follows:

$$\text{Glacier area change per year} = \frac{\text{GA}_a - \text{GA}_b}{n} \tag{2}$$

$$\text{Change in \% of glacier area} = \frac{\text{GA}_a - \text{GA}_b}{\text{GA}_a} \times 100 \tag{3}$$

where GA represents the total glacial coverage (square kilometres), a and b correspond to the starting and ending year, respectively, and n represents the count of years between the starting year and the ending year.

4. RESULTS AND DISCUSSION

4.1. Mapping of Glaciers' surface area

The glaciers' surface area mapping was firstly conducted for the year 2015 for better comparison with RGI v5.0. A weighted coefficient of 0.5 combined with a threshold value of 2.5 emerged as the most suitable values for obtaining clean glaciers from the comparison with RGI v5.0 and a finer resolution of Google Earth image. The land slope of less than 10° and the land surface temperature of 280.64–295.79 K showed the best results for extracting debris-covered glaciers upon the comparison with RGI v5.0 and sharp Google Earth image. The comparison map of generated glacier map for the year 2015 and RGI v5.0 map is shown in Figure 3. The highlighted circle in Figure 3 shows the glacier which was missing in RGI v5.0. The presence of this missing glacier was also found in Google Earth image, leading to the conclusion of the existence of this particular glacier. Figure 4 shows the existence of missing glacier from RGI v5.0 in Google Earth image.

The same process was carried out for the years 2006 and 1994. The weighted coefficient and the threshold value for delineating clean glaciers and the slope of land for obtaining debris-covered glaciers remained same as the year 2015, whereas the land surface temperature was 277.44–299.62 K for the year 2006 and 265.14–287.36 K for the year 1994. The glacier maps of 2006 and 1994 are shown in Figure 5, and the glacier number was cited in the year 1994 map.

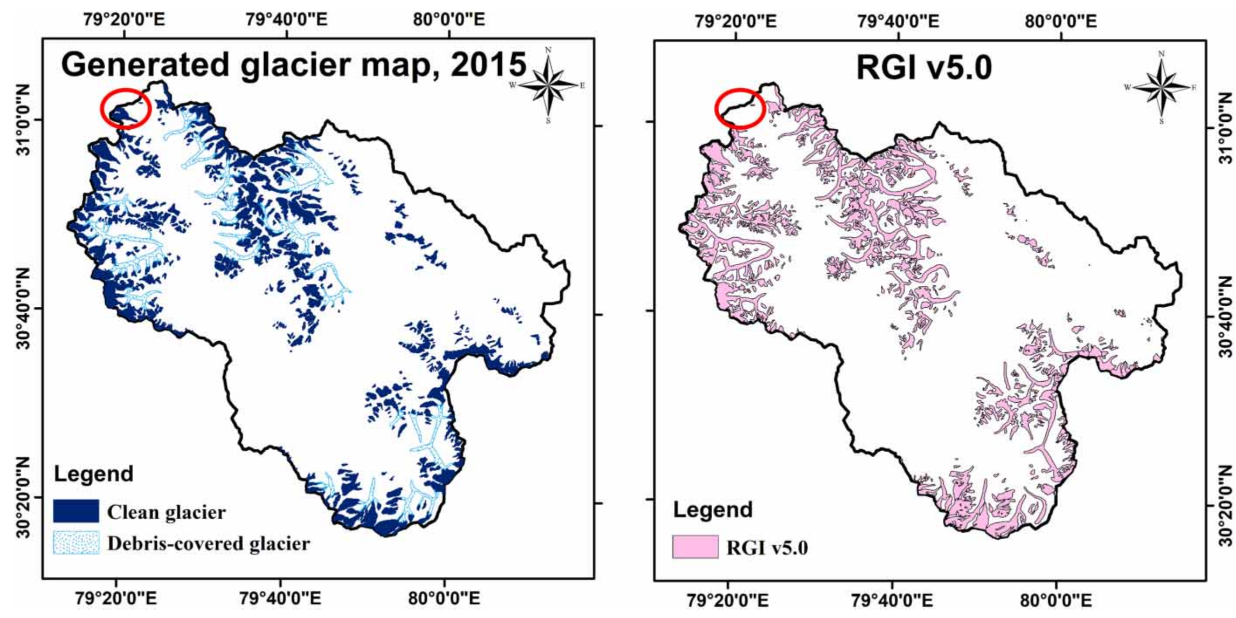

Figure 3 | Comparison of generated glacier map of 2015 and RGI v5.0 map.

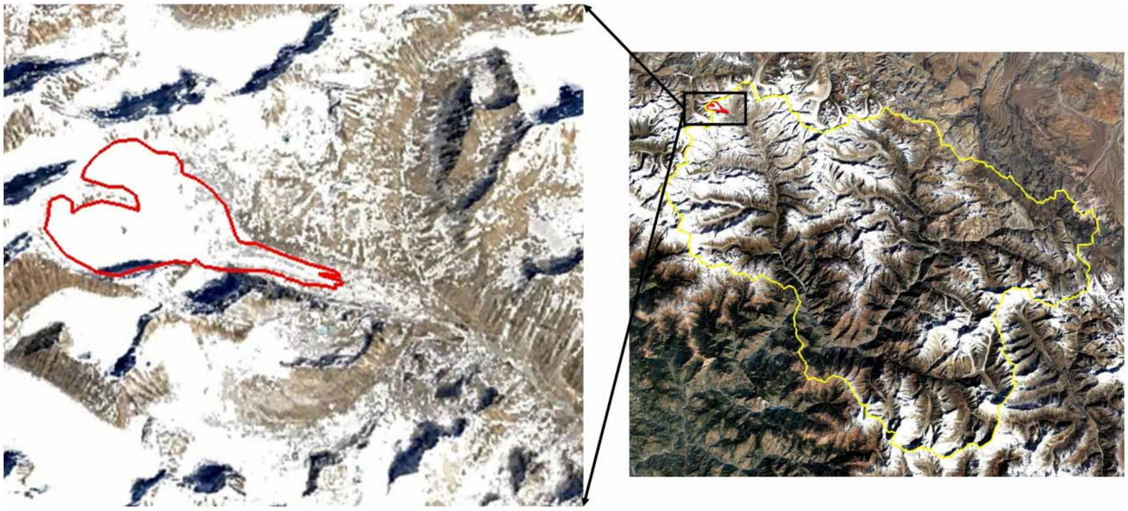

Figure 4 | Highlighting missing glacier in RGI v5.0 in Google Earth image.

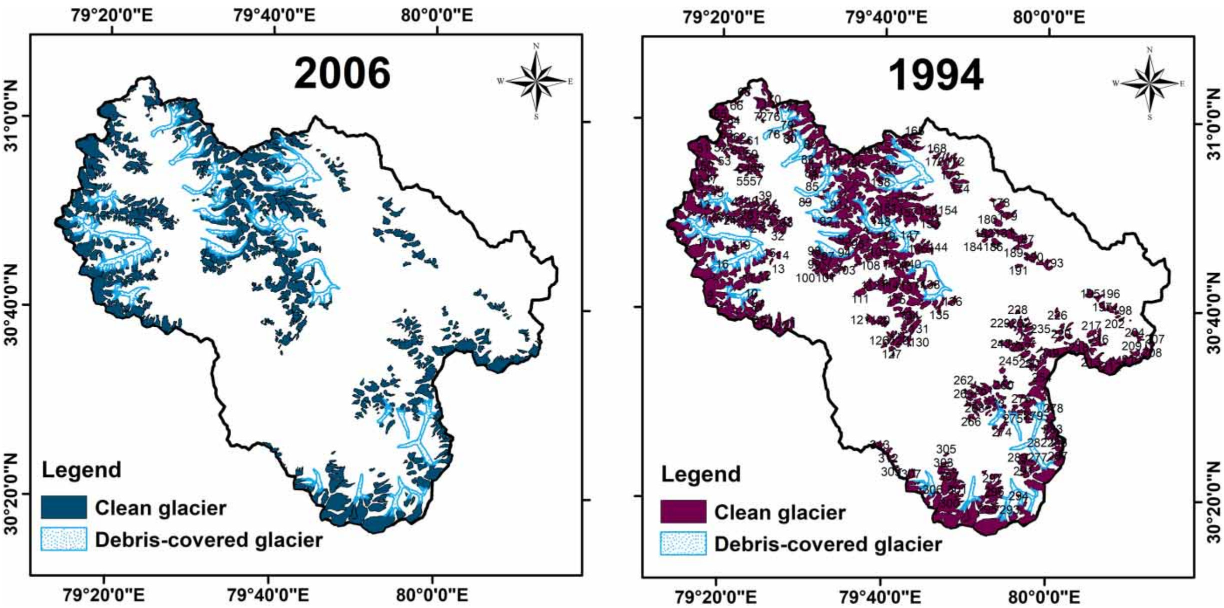

Figure 5 | Generated glacier maps for the years 2006 and 1994.

4.2. Inventory of glaciers

In the year 1994, a tally of 314 glaciers was identified, covering a total area of 1,150.471 km^2 and occupying 25.56% of the total basin; in the year 2006, a total of 340 number of glaciers were recognized, covering a total area of 1,033.955 km^2, which accounted for 22.97% of the entire basin area; and in the year 2015, 360 glaciers were identified, collectively covering an area of 783.107 km^2 and occupying 17.40% of the entire basin area. The decrease in the glacial surface extent was observed, whereas the number of glaciers was increasing, and this is nothing but due to the fragmentation of the individual glaciers. The fragmented glaciers were assigned as A, B, and so on depending on the number of glaciers that got detached from the main glacier. The glacier reduction was 10.128% (116.516 km^2) with an annual reduction rate of 0.78% during the analysis period of 1994–2006; 24.261% (250.848 km^2) glacial shrinkage at the shrinkage rate of 2.43% per annum was observed during 2006–2015; and 31.932% (367.364 sq. km) glacial shrinkage at the rate of 1.45% per annum was observed during 1994–2015 (Table 2). The rate of shrinkage was noted to be higher in the recent periods than that in the older periods. This could suggest that glacier surface extent is notably influenced by the climate change. Tables 3 and 4 present the individual glacier number

Table 2 | Total glacier area, glacier loss, and glacier retreating rate

Glacier area			Glacier area changes				
Year	No. of glaciers	Total glacier area (km^2)	Time interval	Glacier loss km^2	Retreating rate %	km^2/year	%/year
1994	314	1,150.471	1994–2006	116.516	10.128	8.963	0.78
2006	340	1,033.955	2006–2015	250.848	24.261	25.085	2.43
2015	360	783.107	1994–2015	367.364	31.932	16.698	1.45

and area. Some of the small-sized glaciers usually less than 0.5 km^2 in the year 1994 were observed to be exhausted by the year 2015. The analysis periods 1994–2006 showed nine diminished glaciers (G37, G69, G126, G136, G183, G184, G185, G203, and G248), and their sizes varied from 0.07 to 1.46 km^2 with an average size of 0.54 km^2. The periods 2006–2015 showed 16 diminished glaciers (G48, G78, G81, G85, G142, G161, G166, G194, G195, G228, G272, G294, G305, G308, G310, and G314), and their sizes varied from 0.07 to 1.13 km^2 with an average size of 0.27 km^2. G136 and G195 were the only diminished glaciers whose sizes were greater than 1 km^2, this could be due to the location, landscape, and orientation of the glaciers. The smallest size of the glaciers was observed to be 0.072, 0.066, and 0.023 km^2 in the years 1994, 2006, and 2015, respectively, and the maximum size of the glaciers was found to be 71.467, 69.505, and 54.044 km^2 in the year 1994, 2006, and 2015, respectively. The average size of glaciers was observed to be 3.67, 3.06, and 2.20 km^2 in the years 1994, 2006, and 2015. Figure 6 shows an example retreating glaciers (G180 and G197), fragmented glaciers (G191 and G243), and diminished glaciers (G136, G183, and G184) in the Google Earth image by setting the image date at the nearest possible to the acquisition date of Landsat 8 OLI (2015).

The glacial extent based on their sizes was also analysed. The glaciers were categorized into six groups, namely, <0.5, 0.5–1, 1–3, 3–5, 5–10, and >10 km^2. Table 5 provides the details of counts of glaciers and the total area covered under each size group. The maximum glacial coverage was observed in the category of size >10 km^2 for all 3 years, and the minimum extent was observed in the category of <0.5 km^2 for the years 1994 and 2006, whereas 0.5–1 km^2 category showed minimum glacial total coverage for the year 2015. The category of <0.5 km^2 showed an increase in both the count of glaciers and their total coverage for all the 3 years, attributed to the fragmentation and/or reduction of larger-sized glaciers into smaller ones. In the category of 0.5–1 km^2, number of glaciers increased from 1994 to 2006 and then again decreased in the year 2015. The category of 1–3, 3–5, 5–10, and >10 km^2 showed a reduction in glacier numbers and glacial area coverage. The highest count of glaciers was observed in the 1–3 km^2 group in the year 1994 and <0.5 km^2 in the years 2006 and 2015. The minimum number of glaciers was found in the category of >10 km^2 in the years 1994 and 2006, and 3–5 km^2 in the year 2015. The glacial loss based on their sizes (Table 6) was also analysed and the category of 5–10 km^2 showed the highest deglaciation percentage during 1994–2006 and the category of 3–5 km^2 showed the highest deglaciation percentage during 2006–2015 and 1994–2015. The glacier size of <1 km^2 showed an increase in the glacial extent due to a reduction in the higher size group glaciers and adding the glacial extent for the small-sized category.

The glacier area distribution on the different elevation ranges was also analysed. The average elevation of each glacier was determined from DEM and assigned into a different range accordingly. Table 7 shows the count of glaciers and total glacier area under the specific elevation range. The elevation range of 5,000–5,500 m showed the highest number of glaciers and glacial extent in all the analysis periods. The lowest elevation range (4,000–4,500 m) showed a reduction in glacier number and glacial area coverage from 1994 to 2015. The 4,500–5,000 m range showed an increase in glacier numbers from 1994 to 2006 and then decreased from 2006 to 2015. The range of 5,000–5,500 m showed an increase in number of glaciers from 1994 to 2015 and a decrease in glacial area. The elevation range of 5,500–6,000 m showed an increase in the number of glaciers and a decrease in the glacial area. The elevation range of 6,000–6,500 m and >6,500 m showed an increase in glacier number and a reduction in the glacial area from 1994 to 2015.

A total number of 21 glaciers are covered with debris at their frontal areas for all the three years, i.e., 1994, 2006, and 2015. The debris covered was present in the trunk of a large-sized glacier. The increase in the debris-covered glaciers was observed during 1994–2006 by 9.49% and then retreated in the recent periods 2006–2015. The overall analysis period (1994–2015) showed retreating debris covered at the rate of 0.59% per annum (Table 8).

As the reduction in glacier surface area was observed in the study area, it indicated the melting of glaciers. Glacial meltwater is a crucial source of freshwater in the region, and a reduction in glacier surface area will lead to decreased

Table 3 | Individual glacier number and area from G1 to G150

Glacier no.	1994	2006	2015	Glacier no.	1994	2006	2015	Glacier no.	1994	2006	2015	Glacier no.	1994	2006	2015	Glacier no.	1994	2006	2015
G1	1.56	1.11	0.07	G27(B)		0.14	0.12	G58(B)		0.25	0.23	G91(C)			1.96	G119	0.61	0.28	0.24
G2	1.72	0.65	0.13	G27(C)		2.30	1.68	G59(A)	3.38	1.49	0.66	G92(A)	15.96	14.59	10.95	G120(A)	2.04	0.18	0.16
G3	4.71	4.43	1.16	G28	9.00	8.76	6.69	G59(B)		1.43	0.51	G92(B)			12.77	G120(B)		0.25	0.20
G4	2.16	1.52	0.92	G29	0.35	0.32	0.25	G59(C)			0.97	G93	16.17	15.60	0.30	G120(C)		0.17	0.07
G5(A)	4.09	3.05	1.11	G30	1.75	1.73	1.38	G60	5.29	3.96	2.19	G94	0.51	0.31	0.55	G120(D)		0.18	0.13
G5(B)			1.05	G31(A)	2.70	1.65	1.11	G61	0.91	0.83	0.26	G95	0.70	0.57	0.51	G121	1.95	0.18	0.09
G6	0.24	0.21	0.18	G31(B)		0.64	0.44	G62	1.97	1.79	1.12	G96	0.66	0.55	1.25	G122	0.55	0.43	0.30
G7	1.42	0.82	0.54	G32	1.80	1.36	0.80	G63	4.89	4.74	3.39	G97(A)	27.95	25.97	20.99	G123	0.35	0.29	0.18
G8	1.00	0.84	0.69	G33(A)	1.31	0.15	0.11	G64	1.30	1.18	0.72	G97(B)			0.19	G124	0.55	0.26	0.16
G9(A)	44.50	41.75	36.45	G33(B)		0.56	0.42	G65	8.94	8.89	6.13	G98	1.23	0.91	2.81	G125	0.48	0.37	0.20
G9(B)		0.48	0.35	G34(A)	0.89	0.14	0.11	G66	0.37	0.27		G99	3.14	2.96	0.28	G126	0.70		
G9(C)		1.68	0.77	G34(B)		0.26	0.19	G67	0.17	0.17	0.15	G100	1.23	1.01	0.70	G127	0.76	0.17	0.08
G10	1.03	0.63	0.44	G35	0.65	0.13	0.13	G68	0.72	0.59		G101	2.10	1.22	0.53	G128	0.27	0.26	
G11(A)	5.24	3.72	2.97	G36	1.07	0.95	0.64	G69	0.22			G102	0.93	0.69	0.67	G129	4.74	3.65	2.53
G11(B)		1.23	0.68	G37	0.10	0.09		G70	3.63	3.62	2.87	G103	1.02	0.92	0.18	G130	1.31	0.79	0.77
G12(A)	2.22	0.58	0.43	G38	3.08	3.06	2.20	G71	3.72	3.65	2.89	G104	0.72	0.31	0.14	G131	3.25	2.48	1.98
G12(B)		0.89		G39(A)	1.90	1.06	0.39	G72	0.44	0.40	0.27	G105	0.28	0.26	0.27	G132	1.42	0.83	0.61
G13	0.47	0.41	0.36	G39(B)		0.72		G73	0.36	0.29	0.26	G106	0.72	0.27	0.42	G133	0.39	0.37	0.27
G14	0.93	0.62	0.33	G40	3.49	2.67	1.79	G74	0.28	0.26	0.24	G107	0.81	0.70	0.14	G134(A)	4.50	4.49	0.83
G15	1.13	0.87	0.18	G41	1.68	1.63	1.06	G75	0.24	0.22	0.19	G108(A)	1.21	0.68	0.43	G134(B)			1.20
G16(A)	38.81	37.74	29.60	G42	0.61	0.53	0.33	G76	0.71	0.64	0.49	G108(B)			0.57	G134(C)			1.15
G16(B)			0.25	G43	26.60	25.79	18.66	G77	22.67	22.24	18.64	G109(A)	6.32	0.93	1.01	G135	0.93	0.79	0.11
G16(C)			0.22	G44	0.48	0.40	0.36	G78	0.11	0.07		G109(B)		1.71	0.48	G136	1.46		
G16(D)			0.12	G45	1.05	0.98	0.67	G79	0.94	0.88	0.68	G109(C)		0.80	2.70	G137	36.08	35.05	27.23
G16(E)			0.33	G46	7.87	7.62	5.11	G80(A)	1.04	0.70	0.55	G110(A)	4.19	4.18	0.10	G138	0.96	0.59	0.39
G17	47.64	47.26	35.98	G47	3.35	3.28	2.09	G80(B)		0.20	0.11	G110(B)			0.12	G139	0.40	0.38	0.24
G18	0.43	0.36	0.28	G48	0.28	0.24		G81	0.10	0.09		G111	2.23	0.21	0.07	G140(A)	0.64	0.42	0.37
G19	0.72	0.54	0.35	G49	0.41	0.40	0.24	G82	26.87	25.82	22.18	G112(A)	3.65	0.32	0.47	G140(B)		0.19	0.17
G20	2.12	2.10	1.74	G50	6.96	6.66	4.29	G83	1.54	1.48	1.13	G112(B)		0.16		G141	0.42	0.35	0.34
G21	0.71	0.68	0.68	G51	13.86	13.65	9.86	G84	1.55	1.13	0.80	G112(C)		1.10	0.31	G142	0.46	0.25	
G22(A)	0.57	0.50	0.23	G52(A)	2.31	2.23	0.61	G85	0.15	0.14		G113	0.88	0.48	0.68	G143	0.58	0.50	0.33
G22(B)			0.21	G52(B)			1.04	G86	0.96	0.59	0.41	G114(A)	9.32	7.84	0.93	G144	2.17	1.42	0.82

(*Continued.*)

Table 3 | Continued

Glacier no.	1994	2006	2015	Glacier no.	1994	2006	2015	Glacier no.	1994	2006	2015	Glacier no.	1994	2006	2015	Glacier no.	1994	2006	2015
G23(A)	0.46	0.42	0.20	G53	1.19	0.99	0.51	G87(A)	28.77	27.30	24.11	G114(B)			0.23	G145	2.47	2.37	2.30
G23(B)			0.19	G54(A)	3.66	3.56	2.60	G87(B)			0.42	G114(C)			0.17	G146	0.48	0.23	0.23
G24	0.65	0.47	0.41	G54(B)			0.63	G88	0.45	0.37	0.20	G114(D)			0.94	G147	0.42	0.38	0.19
G25	0.50	0.40	0.39	G55	0.40	0.38	0.36	G89	0.17	0.14	0.13	G115	4.42	3.04	0.58	G148(A)	61.27	57.81	48.05
G26(A)	0.60	0.16	0.15	G56	0.46	0.43	0.39	G90	0.13	0.11	0.10	G116	1.25	0.71	0.55	G148(B)		0.35	0.42
G26(B)		0.17	0.17	G57	1.80	1.56	1.40	G91(A)	16.42	14.77	9.20	G117	1.41	0.92	0.11	G149	0.19	0.17	0.16
G27(A)	3.56	0.38	0.19	G58(A)	2.19	1.88	1.18	G91(B)			0.58	G118	0.48	0.14		G150	0.95	0.35	0.32

Table 4 | Individual glacier number and area from G151 to G314

Glacier no.	1994	2006	2015	Glacier no.	1994	2006	2015	Glacier no.	1994	2006	2015	Glacier no.	1994	2006	2015	Glacier no.	1994	2006	2015
G151	0.36	0.21	0.18	G183	0.81			G214(B)			0.75	G249	6.56	6.46	6.03	G285(A)	2.09	1.85	0.44
G152(A)	9.88	7.92	0.44	G184	0.67			G215	0.44	0.31	0.22	G250(A)	2.48	2.40	0.44	G285(B)			0.95
G152(B)			7.34	G185	0.36			G216(A)	3.65	3.40	1.09	G250(B)			0.75	G286	1.16	0.97	0.63
G153(A)	5.69	1.84	0.36	G186	1.57	0.52	0.30	G216(B)			0.34	G251	0.31	0.30	0.27	G287	1.53	1.35	0.58
G153(B)		2.53	0.93	G187	3.15	3.04	1.86	G217	1.68	1.43	0.36	G252	0.62	0.55	0.22	G288	0.42	0.32	0.10
G153(C)			1.91	G188	0.86	0.67		G218	7.53	7.49	6.52	G253	0.35	0.32	0.27	G289	2.14	1.62	1.27
G154	1.03	0.35	0.35	G189	1.78	1.73	0.94	G219	0.37	0.29	0.09	G254	8.55	6.40	5.04	G290	0.41	0.32	0.23
G155(A)	9.67	0.14	1.60	G190	3.24	2.94	2.61	G220	1.12	1.08	0.51	G255	1.01	0.75	0.18	G291	1.48	1.28	0.43
G155(B)		0.20	3.72	G191(A)	0.88	0.76	0.52	G221(A)	1.03	0.86	0.24	G256	0.33	0.24	0.15	G292	1.44	1.09	0.67
G155(C)		2.18		G191(B)			0.09	G221(B)			0.07	G257	1.60	1.36	0.93	G293(A)	45.69	0.71	35.21
G155(D)		4.46		G192	0.80	0.77	0.61	G222	0.96	0.89	0.42	G258	0.44	0.43	0.31	G293(B)		42.49	0.56
G156	5.05	4.04	2.20	G193	1.28	0.95	0.52	G223	0.38	0.36	0.13	G259	1.26	1.04	0.76	G293(C)		0.69	0.45
G157(A)	71.47	69.51	54.04	G194	0.75	0.43		G224	0.53	0.37	0.11	G260	2.05	1.79	1.70	G293(D)		0.67	
G157(B)		0.34	0.21	G195	1.97	1.13		G225	0.63	0.55	0.31	G261	4.42	4.29	3.95	G294	0.24	0.20	
G158	0.27	0.22	0.20	G196(A)	1.24	0.70	0.07	G226	0.72	0.68	0.25	G262	0.69	0.56	0.23	G295	4.55	4.35	3.28
G159	0.52	0.45	0.40	G196(B)			0.14	G227(A)	0.48	0.38	0.08	G263	2.17	1.83	1.75	G296	4.16	3.72	3.32
G160	2.53	2.41	1.93	G197	1.45	1.07	0.67	G227(B)			0.02	G264	0.78	0.64	0.33	G297	2.67	1.73	1.73
G161	0.40	0.36		G198(A)	1.24	1.14	0.56	G228	0.44	0.24		G265	0.89	0.82	0.43	G298	1.28	0.86	0.23
G162	0.36	0.35	0.27	G198(B)			0.32	G229	1.10	0.83	0.60	G266(A)	1.23	0.26	0.66	G299	0.43	0.41	0.36
G163	0.18	0.15	0.11	G199	0.70	0.58	0.20	G230	0.34	0.29	0.21	G266(B)		0.89	0.17	G300	43.36	40.92	30.24
G164	4.92	4.32	2.49	G200	0.46	0.31	0.09	G231	0.36	0.34	0.32	G267	0.62	0.56	0.48	G301	3.04	2.39	1.74
G165	0.95	0.84	0.48	G201(A)	0.37	0.31	0.11	G232	1.66	1.55	1.41	G268(A)	2.83	2.39	0.90	G302	9.13	8.97	6.94
G166	0.16	0.11		G201(B)			0.07	G233	0.30	0.22	0.15	G268(B)			0.65	G303(A)	2.82	2.21	1.45
G167	0.26	0.20	0.17	G202	0.47	0.28	0.20	G234	0.65	0.53	0.32	G269	0.52	0.51	0.35	G303(B)		0.54	
G168	1.04	0.50	0.32	G203	0.07			G235	1.32	1.15	0.84	G270	0.44	0.16	0.12	G304	0.68	0.51	0.36
G169	0.92	0.62	0.31	G204	1.12	1.02	0.56	G236	0.88	0.72	0.45	G271	0.13	0.08	0.05	G305	0.44	0.25	
G170	2.08	0.96	0.68	G205	0.44	0.42	0.21	G237	0.33	0.30	0.29	G272	0.31	0.28		G306	15.45	14.78	10.99
G171	0.56	0.27	0.22	G206(A)	0.67	0.48	0.16	G238	0.56	0.55	0.29	G273(A)	9.58	9.33	7.16	G307(A)	2.38	1.72	0.40
G172	2.69	0.52	0.47	G206(B)			0.08	G239	0.48	0.45	0.29	G273(B)			0.13	G307(B)			0.35
G173	2.78	2.49	1.71	G207	0.30	0.24	0.24	G240	0.10	0.09	0.06	G274	1.91	1.89	1.59	G307(C)			0.46
G174	1.97	0.51	0.33	G208	2.92	2.84	1.47	G241	0.70	0.65	0.37	G275	6.55	6.08	4.93	G308	0.19	0.11	
G175(A)	1.66	0.64	0.49	G209	1.32	0.71	0.71	G242(A)	6.49	6.19	2.91	G276	1.05	0.84	0.28	G309	0.37	0.29	0.08

(*Continued.*)

Table 4 | Continued

Glacier no.	1994	2006	2015	Glacier no.	1994	2006	2015	Glacier no.	1994	2006	2015	Glacier no.	1994	2006	2015	Glacier no.	1994	2006	2015
G175(B)		0.26	0.24	G210(A)	3.34	2.89	0.33	G242(B)			1.31	G277(A)	43.84	41.42	36.96	G310	0.44	0.19	
G176(A)	1.12	1.03	0.17	G210(B)			0.69	G242(C)			1.30	G277(B)			0.22	G311	0.70	0.67	0.22
G176(B)			0.43	G211	0.68	0.68	0.24	G243(A)	1.87	1.52	0.71	G278	0.64	0.57	0.34	G312	0.89	0.68	0.22
G177	0.55	0.49	0.30	G212(A)	8.55	8.14	0.53	G243(B)			0.28	G279	0.75	0.56	0.39	G313	1.31	0.73	0.26
G178	2.31	2.15	1.63	G212(B)			0.97	G244	0.34	0.30	0.30	G280	0.51	0.44	0.28	G314	0.32	0.21	
G179	2.69	2.41	0.69	G212(C)			1.65	G245	1.66	1.58	0.82	G281	0.86	0.74	0.31				
G180	2.00	1.58	1.49	G212(D)			2.48	G246	0.20	0.20	0.19	G282	1.76	1.65	1.29				
G181	5.13	3.38	2.65	G213	5.83	5.55	5.50	G247	1.22	1.08	0.50	G283	1.82	1.43	0.61				
G182	3.06	2.18	2.11	G214(A)	1.07	1.05	0.19	G248	0.45			G284	0.31	0.26	0.22				

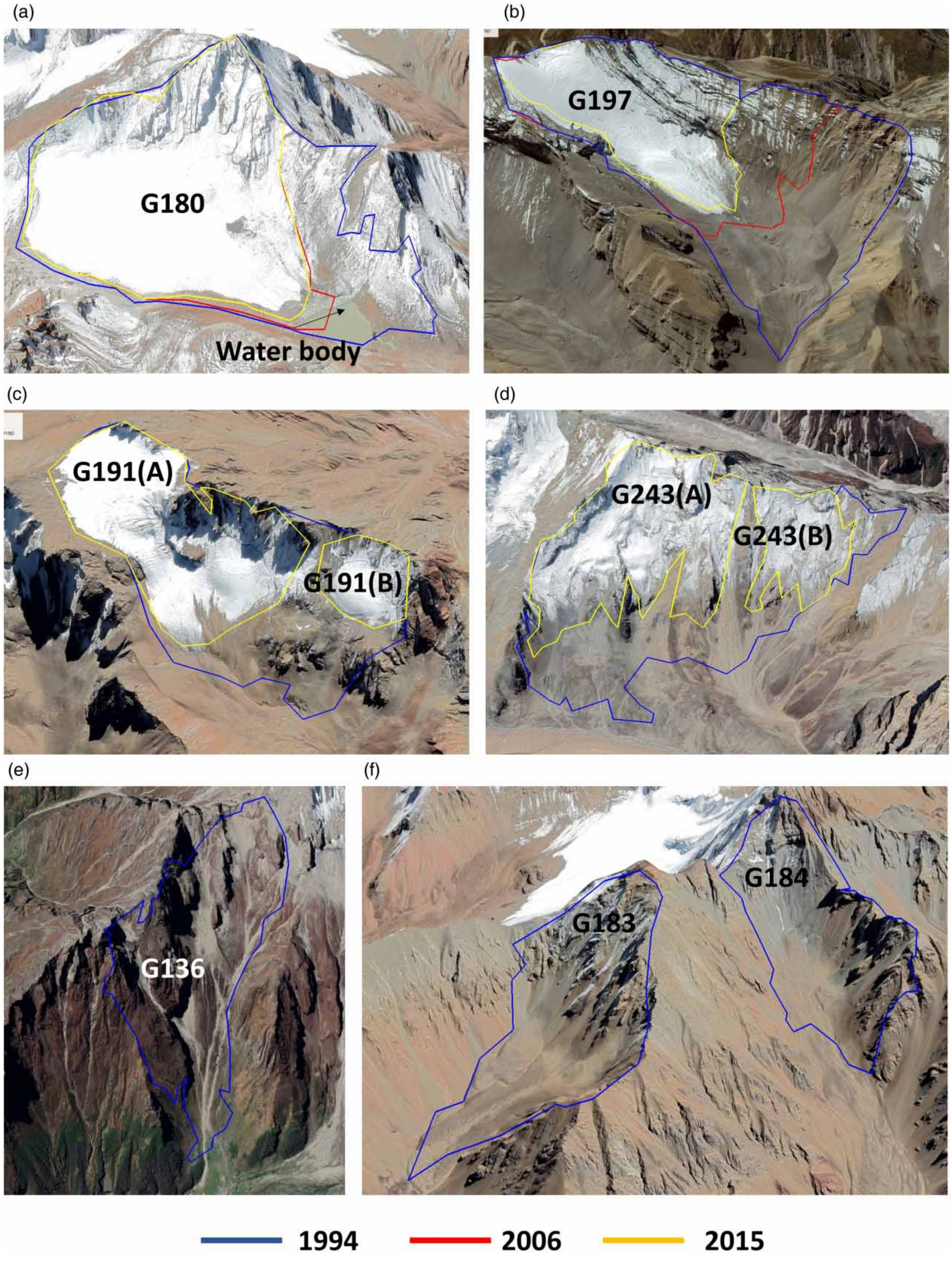

Figure 6 | (a and b) Retreating glaciers of G180 and G197, (c and d) fragmented glaciers of G191 and G243 from 1994 to 2015, (e and f) diminished glaciers of G136, G183, and G184 in Google Earth image.

meltwater contribution to the streams. The reduction in glacial meltwater contributions can alter the hydrological regime in the region, thus affecting water availability during dry periods. The melting of glaciers also contributes to the formation, growth, and expansion of glacial lakes, and can cause sudden and catastrophic release of water to the downstream region,

Table 5 | Number of glaciers and its coverage based on their sizes

	1994		2006		2015	
Size (km^2)	No. of glaciers	Area (km^2)	No. of glaciers	Area (km^2)	No. of glaciers	Area (km^2)
<0.5	83	28.215	124	34.554	197	49.778
0.5–1	67	49.282	86	60.881	67	45.691
1–3	95	160.588	73	125.556	61	109.907
3–5	28	106.949	23	86.606	7	28.055
5–10	22	163.03	15	111.6	11	76.486
>10	19	643.119	19	615	18	473.188

Table 6 | Glacial loss based on the size category

	Glacier loss percentage during the respective time interval based on their size		
Glacier size (km^2)	1994–2006	2006–2015	1994–2015
<0.5	−22.47	−30.58	−76.42
0.5–1	−23.53	24.95	7.29
1–3	21.81	12.46	31.56
3–5	19.02	67.61	73.77
5–10	31.55	31.46	43.08
>10	4.27	23.06	26.34

Table 7 | Glaciers distribution based on elevation range

	1994		2006		2015	
Elevation range (m)	No. of glaciers	Total glacier area (km^2)	No. of glaciers	Total glacier area (km^2)	No. of glaciers	Total glacier area (km^2)
4,000–4,500	7	9.313	1	1.114	1	0.47
4,500–5,000	48	95.458	55	65.368	51	134.541
5,000–5,500	143	584.573	154	576.341	175	457.374
5,500–6,000	110	454.517	124	385.955	125	184.844
6,000–6,500	5	4.079	5	2.768	6	1.983
>6,500	1	2.531	1	2.409	2	3.895

Table 8 | Reduction of debris-covered glaciers

Debris-covered glacier area		Debris-covered glacier area changes				
Year	Total area (km^2)	Time interval	Glacier loss (km^2)	%	Retreating rate km^2/year	%/year
1994	192.54	1994–2006	−18.28	−9.49	−1.41	−0.73
2006	210.82	2006–2015	43.13	20.46	4.31	2.05
2015	167.69	1994–2015	24.85	12.91	1.13	0.59

which is known as glacier lake outburst flood (GLOF). It can lead to flash floods with loss of lives, destruction of infrastructures, and alterations to downstream ecosystems. The challenges mentioned are predominantly associated with the retreat of glaciers, and hence analysing and monitoring the glacier surface extent at regular intervals are necessary.

5. CONCLUSIONS

This study presented detailed glacier inventory in the whole Alaknanda River basin (outlet at Joshimath) using Landsat series data, land surface temperature, and DEM for the period between 1994 and 2015. The glacier maps of 1994, 2006, and 2015 were prepared, and the temporal variations in glacier surface was analysed. It was observed that the glacier surface extent was reduced by 367.364 km^2 during the study period at the shrinkage rate of 1.45% per annum. Upon dividing the time period as recent (2006–2015) and old (1994–2006) periods, the recent periods showed a higher deglaciation rate that may imply the impact of increasing the magnitude of climate warming. The debris-covered glacier was reduced at the rate of 0.59% per annum from 1994 to 2015. The increase in the count of glaciers was also observed due to the fragmentation of individual glaciers. The glacier surface area occupied about 25% of the total basin in the year 1994, whereas it occupied about only 17% in the year 2015. The elevation range of 5,000–5,500 m above m.s.l. hosted a maximum number of glaciers and glacial coverage. It is believed that the glacier map prepared in the present study will be helpful for the hydrologist/modeller to quantify the proportion of glacier melt to the total stream runoff at the Joshimath, where CWC measures daily discharge which will eventually be useful in analysing the hydrological regime for water management, security, and sustainability in the region.

ACKNOWLEDGEMENTS

The authors gratefully acknowledge the help, encouragement, and financial support provided by the Climate Change Programme (CCP), Strategic Programmes, Large Initiatives and Coordinated Action Enabler (SPLICE), Department of Science and Technology, Government of India under National Network Programme on Himalayan Cryosphere as part of National Mission on Sustaining Himalayan Ecosystem (NMSHE) through Grant Nos. DST/CCP/NHC/154/2018 and DST/CCP/MRDP/184/2019.

DECLARATIONS

All authors have read, understood, and have complied as applicable with the statement on "Ethical responsibilities of Authors" as found in the Instructions for Authors and are aware that with minor exceptions, no changes can be made to authorship once the paper is submitted.

FUNDING

The authors gratefully acknowledge the help, encouragement, and financial support provided by the CCP, SPLICE, Department of Science and Technology, Government of India under National Mission on Sustaining Himalayan Ecosystem (NMSHE) through Grant Nos. DST/CCP/NHC/154/2018 and DST/CCP/MRDP/184/2019.

AUTHORS' CONTRIBUTIONS

V. Nunchhani: methodology (debris-covered glaciers) and manuscript preparation. Sujit Hazarika: data acquisition, data preparation, and methodology. Rimum Murtem: methodology (clean glaciers). Arnab Bandyopadhyay: supervision, manuscript editing, communicating, and grant recipient. Aditi Bhadra: conceptualization, supervision, visualization, manuscript revision, and grant recipient.

DATA AVAILABILITY STATEMENT

All relevant data are included in the paper or its Supplementary Information.

CONFLICT OF INTEREST

The authors declare there is no conflict.

REFERENCES

Aggarwal, K. C., Kumar, V. & Dass, T. 1983 Snowmelt run-off for a catchment of Beas basin. In: *Proceedings of the First National Symposium on Seasonal Snow Cover, SASE*, 28–30 April, Manali, India, pp. 43–63.

Alam, M. & Bhardwaj, S. 2020 Temporal variation in glacier's area and identification of glacial lake in Sikkim. In: Geoecology of Landscape Dynamics. Advances in Geographical and Environmental Sciences (Sahdev, S., Singh, R., Kumar, M., eds.). Springer, Singapore. doi: 10.1007/978-981-15-2097-6_8.

Alifu, H., Johnson, B. A. & Tateishi, R. 2016 Delineation of debris-covered glaciers based on a combination of geomorphometric parameters and a TIR/NIR/SWIR band ratio. *IEEE Journal of Selected Topics in Applied Earth Observations and Remote Sensing* **9** (2), 781–792. https://doi.org/10.1109/JSTARS.2015.2500906.

Azam, M. F., Kargel, J. S., Shea, J. M., Nepal, S., Haritashya, U. K., Srivastava, S., Maussion, F., Qazi, N., Chevallier, P., Dimri, A. P., Kulkarni, A. V., Cogley, J. G. & Bahuguna, I. 2021 Glaciohydrology of the Himalya-Karakoram. *Science* **373** (6557). https://doi.org/10.1126/science.abf3668.

Bajracharya, S. R., Mool, P. R. & Shrestha, B. R., 2008 Global climate change and melting of Himalayan glaciers. In: *Melting Glaciers and Rising Sea Levels: Impacts and Implications* (Ranade, P. S., ed.). The Icfai's University Press, India, pp. 28–46.

Benn, D. I., Bolch, T., Hands, K., Gulley, J., Luckman, A., Nicholson, L. I., Quincey, D., Thompson, S., Toumi, R. & Wiseman, S. 2012 Response of debris-covered glaciers in the Mount Everest region to recent warming, and implications for outburst flood hazards. *Earth-Science Reviews* **114** (1–2), 156–174. https://doi.org/10.1016/j.earscirev.2012.03.008.

Bhambri, R., Bolch, T., Chaujar, R. K. & Kulshreshtha, S. C. 2011 Glacier changes in the Garhwal Himalaya, India, from 1968 to 2006 based on remote sensing. *Journal of Glaciology* **57** (203), 543–556. https://doi.org/10.3189/002214311796905604.

Bolch, T. & Kamp, U. 2006 Glacier mapping in high mountains using DEMs, Landsat and ASTER data. *Grazer Schriften Der Geographie Und Raumforschung* **1**, 37–48. Available from: http://web.unbc.ca/~bolch/publications/BolcKamp06_GeoRaum.pdf.

Bolch, T., Buchroithner, M., Kunert, A. & Kamp, U. 2007 Automated Delineation of Debris-Covered Glaciers Based on ASTER Data. Geoinformation in Europe (Proc. of 27th EARSel Symposium, 4–7 June 2007), Bozen, Italy, June, 403–410. Available from: citeulike-article-id:9343684%5Cnhttp://web.unbc.ca/~bolch/publications/BolchAl07_EARSeL-iPr.pdf.

Bolch, T., Kulkarni, A., Kääb, A., Huggel, C., Paul, F., Cogley, J. G., Frey, H., Kargel, J. S., Fujita, K., Scheel, M., Bajracharya, S. & Stoffel, M. 2012 The state and fate of Himalayan glaciers. *Science* **336** (6079), 310–314. https://doi.org/10.1126/science.1215828.

Bolch, T., Pieczonka, T., Mukherjee, K. & Shea, J. 2017 Brief communication: Glaciers in the Hunza catchment (Karakoram) have been nearly in balance since the 1970s. *Cryosphere* **11** (1), 531–539. https://doi.org/10.5194/tc-11-531-2017.

Chand, P. & Sharma, M. C. 2015 Glacier changes in the Ravi basin, North-Western Himalaya (India) during the last four decades (1971–2010/13). *Global and Planetary Change* **135**, 133–147.

Dimri, A. P., Allen, S., Huggel, C., Mal, S., Ballesteros-Canovas, J. A., Rohrer, M., Shukla, A., Tiwari, P., Maharana, P., Bolch, T., Thayyen, R., Stoffel, M. & Pandey, A. 2021 Climate change, cryosphere and impacts in the Indian Himalayan Region. *Current Science* **120** (5), 775–790. doi: 10.18520/cs/v120/i5/774-790.

Garg, P. K., Shukla, A. & Jasrotia, A. S. 2017 Influence of topography on glacier changes in the central Himalaya, India. *Global and Planetary Change* **155**, 196–212. doi: 10.1016/j.gloplacha.2017.07.007.

Immerzeel, W. W., Lutz, A. F., Andrade, M., Bahl, A., Biemans, H., Bolch, T., Hyde, S., Brumby, S., Davies, B. J., Elmore, A. C., Emmer, A., Feng, M., Fernandez, A., Haritashya, U., Kargel, J. S., Koppes, M., Kraaijenbrink, P. D. A., Kulkarni, A. V., Mayewski, P. A., Nepal, S., Pacheco, P., Painter, T. H., Rajaram, H., Rupper, S., Sinisalo, A., Shrestha, A. B., Viviroli, D., Wada, Y., Xiao, C., Yao, T. & Baillie, J. E. M. 2020 Importance and vulnerability of the world's water towers. *Nature* **577** (7790), 364–369.

Kaushik, S., Singh, T., Bhardwaj, A., Joshi, P. K. & Dietz, J. A. 2022 Automated delineation of supraglacial debris cover using deep learning and multisource remote sensing data. *Remote Sensing* **14**, 1352. https://doi.org/10.3390/rs14061352.

Keeler, D. G., Rupper, S. & Schaefer, J. M. 2021 A first-order flexible ELA model based on geomorphic constraints. *MethodsX* **8**, 101173. https://doi.org/10.1016/j.mex.2020.101173.

Kulkarni, A. V., Rathore, B. P. & Alex, S. 2004 Monitoring of glacial mass balance in the Baspa basin using accumulation area ratio method. *Current Science* **86** (1), 185–190.

Kulkarni, A. V., Rathore, B. P., Mahajan, S. & Mathur, P. 2005 Alarming retreat of Parbati glacier, Beas basin, Himachal Pradesh. *Current Science* **88** (11), 1844–1850.

Kulkarni, A. V., Bahuguna, I. M., Rathore, B. P., Singh, S. K., Randhawa, S. S., Sood, R. K. & Dhar, S. 2007 Glacial retreat in Himalaya using Indian remote sensing satellite data. *Current Science* **92** (1), 69–74. https://doi.org/10.1117/12.694004.

Kulkarni, A. V., Rathore, B. P., Singh, S. K. & Bahuguna, I. M. 2011 Understanding changes in the Himalayan cryosphere using remote sensing techniques. *International Journal of Remote Sensing* **32** (3), 601–615. https://doi.org/10.1080/01431161.2010.517802.

Maisch, M., Haeberli, W., Hoelzle, M. & Wenzel, J. 1999 Occurrence of rocky and sedimentary glacier beds in the Swiss Alps as estimated from glacier-inventory data. *Annals of Glaciology* **28**, 231–235.

Mehta, M., Dobhal, D. P. & Bisht, M. P. S. 2011 Change of Tipra glacier in the Garhwal Himalaya, India, between 1962 and 2008. *Progress in Physical Geography* **35** (6), 721–738. https://doi.org/10.1177/0309133311411760.

Mir, R. A., Jain, S. K., Saraf, A. K. & Goswami, A. 2014 Glacier changes using satellite data and effect of climate in Tirungkhad basin located in western Himalaya. *Geocarto International* **29** (3), 293–313. http://dx.doi.org/10.1080/10106049.2012.760655.

Mir, R. A., Jain, S. K., Jain, S. K., Thayyen, R. J. & Saraj, A. K. 2017 Assessment of recent glacier changes and its controlling factors from 1976 to 2011 in Baspa basin, western Himalaya. *Arctic, Antarctic and Alpine Research* **49** (4), 621–647. http://dx.doi.org/10.1657/AAAR0015-070.

Mishra, A., Nainwal, H. C., Bolch, T., Shah, S. S. & Shankar, R. 2023 Glacier inventory and glacier changes (1994–2020) in the Upper Alaknanda Basin, Central Himalaya. *Journal of Glaciology* **69** (275), 591–606. https://doi.org/10.1017/jog.2022.87.

Nainwal, H. C., Banerjee, A., Shankar, R., Semwal, P. & Sharma, T. 2016 Shrinkage of Satopanth and Bhagirath Kharak Glaciers, India, from 1936 to 2013. *Annals of Glaciology* **57** (71), 131–139. https://doi.org/10.3189/2016aog71a015.

Oerlemans, J. 2005 Extracting a climate signal from 169 glacier records. *Science* **308** (5722), 675–677. doi:10.1126/science.1107046.

Padma, T. V. 2020 A future of retreating glaciers in the Himalayas. *Eos* **101**. https://doi.org/10.1029/2020EO147437.

Paul, F., Huggel, C. & Kääb, A. 2004 Combining satellite multispectral image data and a digital elevation model for mapping debris-covered glaciers. *Remote Sensing of Environment* **89** (4), 510–518. https://doi.org/10.1016/j.rse.2003.11.007.

Rai, P. K., Mishra, V. N., Singh, S., Prasad, R. & Nathawat, M. S. 2017 Remote sensing-based study for evaluating the changes in glacial area: A case study from Himachal Pradesh, India. *Earth Systems and Environment*. doi:10.1007/s41748-017-0001-2.

SAC 2011 Snow and Glaciers of the Himalayas (Study Carried out Under the Joint Project of Ministry of Environment and Forests and Department of Space, Government of India); Space Applications Centre, ISRO: Ahmedabad, India: 258.

Shukla, A., Gupta, R. P. & Arora, M. K. 2009 Estimation of debris cover and It temporal variation using optical satellite sensor data: A case study in Chenab Basin, Himalaya. *Journal of Glaciology* **55** (191), 444–452. doi:10.3189/002214309788816632.

Shukla, A., Garg, S., Mehta, M., Kumar, V. & Kant Shukla, U. 2020 Temporal inventory of glaciers in the Suru sub-basin, western Himalaya: Impacts of regional climate variability. *Earth System Science Data* **12** (2), 1245–1265. https://doi.org/10.5194/essd-12-1245-2020.

Suresh, D., Chand, S. M., Krishna, M. M., Marcus, N. & Susanne, S. 2023 Half-a-century (1971–2020) of glacier shrinkage and climate variability in Bhaga basin, western Himalaya. *Journal of Mountain Science.* **20** (2), 299–324. https://doi.org/10.1007/s11629-022-7598-9.

Zemp, M., Frey, H., Gärtnerroer, I., Nussbaumer, S. U., Hoelzle, M., Paul, F., Haeberli, W., Denzinger, F., Ahlstrøm, A. P. & Anderson, B. 2015 Historically unprecedented global glacier decline in the early 21st century. *Journal of Glaciology* **61**, 745–762.

Zhang, M., Wang, X., Shi, C. & Yan, D. 2019 Automated glacier extraction index by optimization of Red/SWIR and NIR/SWIR ratio index for glacier mapping using Landsat imagery. *Water* **11**, 1223. doi:10.3390/w11061223.

First received 8 October 2023; accepted in revised form 22 December 2023. Available online 22 January 2024